Dry Metal Forming Open Access Journal

Fast Manuscript Track

High-speed Direct Laser Interference Patterning of sheet metals for friction reduction in deep drawing processes

Theresa Jähnig*[1], Ali Mousavi[2], Valentin Lang[1,3], Tim Kunze[3], Alexander Brosius[2], Andrés Fabián Lasagni[1,3]

[1] Institute for Manufacturing Technology, Technische Universität Dresden, 01062 Dresden
[2] Institute of Forming Processes, Technische Universität Dresden, 01062 Dresden
[3] Fraunhofer IWS, Institute for Material and Beam Technology, Winterbergstraße 28, 01277 Dresden

Abstract

Friction has a dominant influence on manufacturing processes. In deep drawing of sheet metals, lubricants are regularly used to reduce friction forces. Significant production costs originating from supply, application, removal and disposal as well as the negative environmental consequences of using lubricants promote extended research on lubricant free deep drawing processes and tools. A combination of macro-structuring in the flange area and micro-structuring of ta-C layers at the pulling edge radius of deep drawing tools is identified to compensate the loss of tribological functions. Surface texturing of semi-finished sheet metals supports the friction reduction by minimizing the contact area to the deep drawing tool. In this study, a new concept for sheet metal texturing is presented. Using Direct Laser Interference Patterning, periodic surface patterns are fabricated at high fabrication speeds and their influence on the friction behaviour is tested by means of draw bend test. The results show minimal friction for ta-C covered draw bend tools and sheet metal structuring in bending direction.

Keywords: High-speed structuring, direct laser interference patterning, friction reduction, sheet metal forming, lubricant free forming

1 Introduction

In deep drawing processes, intensive interactions between workpiece and tool surface takes place due to the relative motion of sheet metal under high surface pressure. Moreover and contrary to bulk metal forming, deep drawing processes exhibit only minor contact normal stresses [1]. The tribological conditions can be best described by mixed friction, a combination of solid-, liquid- and cross-friction [2].

Lubricants are typically used to protect the semi-finished products and tools by reducing the friction forces which additionally leads to an enlargement of the process window [3]. Besides the positive technological aspects, numerous negative economic and ecological effects arise from the use of lubricants. The annual consumption of water mixed metal working fluids for the European Union is 5 million tons [4]. Not only the lubricant and its disposal causes relevant economic costs, also the appliance and the removal are time consuming, and therefore cost effective process steps [5 - 7].

First attempts to gradually decrease the amount of necessary lubricants are done by: minimal lubricated forming [8], closed loop systems of deep drawing process [9] and the development of biocompatible lubricants, as a promising strategy to make lubricants more environmental friendly [10].

However, the implementation of a lubricant free deep drawing process by influencing the friction forces and the material flow will be realized by a combination of (1) macro-structuring tool flanges, (2) coating and micro-structuring tool pulling edge radii and (3) micro-structuring semi-finished metal sheets. In the present study, micro structures are fabricated on metal sheets by direct laser interference patterning, DLIP. The resulting topography is analysed by confocal microscope analysis and the change of friction behaviour is detected by draw bend tests.

2   Experimental setup

2.1   Direct laser interference patterning of sheet metals

DLIP enables the fabrication of periodic surface structures on different material surfaces by transferring the shape of interference patterns directly to the treated materials [11–13]. In DLIP, a pulsed laser beam is split into several partial beams and recombined on the material surface. The material can either be photo thermally or photo chemically ablated at the maxima positions [14,15], depending on the used laser system. The periodic surface structures are made in one step, without the necessity of ensuing wet chemical [16,17] or imprinting steps. The local energy distribution of the pattern depends on the number of laser beams, the wavelength λ and the angle θ between the individual beams [18-20].
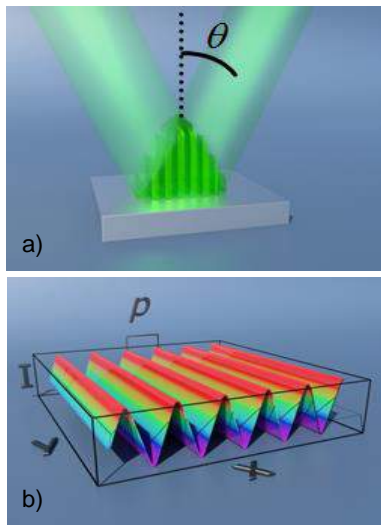

Fig. 1:   a) Overlapping of two laser beams under angle **θ** on the sample surface for DLIP structuring. b) Spatial variation in x- and y-direction of intensity maxima and - minima with the period p.

Using a two-beam configuration (Figure 1a), a line-like energy distribution *I* is obtained, as described by Equation 1:

$$I = 2I_0 \cos(kx \sin\theta)^2 \qquad (1)$$

with I_0 as the laser intensity of each sub-beam, θ as the angle between the beams, and k as the wave number defined as $2\pi/\lambda$. The spatial period *p* (see Figure 1b), defined as the distance between two intensity maxima (or minima) can be calculated using Equation 2:

$$p = \frac{\lambda}{2\sin(\theta)} \qquad (2)$$

DLIP has been successfully used for reducing friction, to produce optical devices as well as for achieving biocompatible enhanced properties or for producing nanoparticles [13–15,19,21].

Compared to other laser surface texturing methods, very high process speeds of up to 0.36 m²/min and 0.9 m²/min to can be reached on metals and polymers using DLIP approaches, respectively [22]. The concept for high speed structuring is adapted to the main DLIP-setup in order to generate functionalized surface structures on the semi-finished metal sheets. The setup of the high-speed DLIP-optical head has been already described elsewhere [23]. The interference pattern is thereby aligned orthogonal to the length of the line-like spot (Figure 2 a, b). The incoming, round laser spot is expanded and formed to a line-like spot (Figure 2 c). The distances between consecutive laser pulses (in both directions) are smaller than the spot diameter, which results in the overlap of the individual pulses. In consequence, the overlap of the pulses implies multiple irradiations of the treated areas, and thereby being a crucial parameter for the entire laser process.
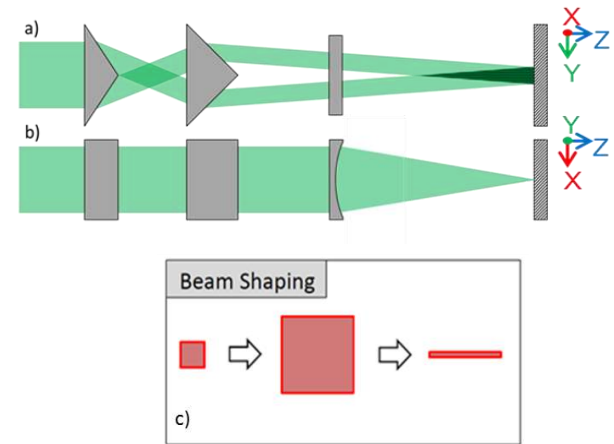

Fig. 2:   Beam shaping and guidance for linear spot shape in top-view a) and side-view b). The beam passes through beam expansion and beam separation. Following the beams are overlapped on the sample surface by passing through a cylindrical collector lens. The spot design is changed from round to line-like c).

The micro structuring of metal sheets was performed with a nanosecond (ns) pulsed laser source with a wavelength of 1064 nm. Moreover, the used laser power was 60.7 W with a repetition rate of 2 kHz. The interference area which is generated by one individual pulse on the material amounts to 0.8 mm² (0.1 mm x 8 mm). Consequently, the line distance (dl) was calculated as a multiple of the spatial period obtaining 80 µm (10 times p = 8 µm) distances.

The micro-structuring was performed on commercially-sourced DC04 steel, cut in strips of 1 mm thickness, 1000 mm length and 20 mm width. Before structuring, the metal strips wee cold-rolled and cleaned using a citrus based cleaner and acetone to remove any pre-lubrication. One set of 42 strips is left unstructured for reference purpose (Figure 3a). Two types of DLIP structures are produced on the other test strips: one set of 42 strips with structures longitudinal (Figure 3b) and one set of 42 strips with structures transverse (Figure 3c) to the bending direction.

The structured area on the metal strips is larger than the area which will be in contact with the bending tool in order to ensure a homogenous surface structure influence during the bending procedure. The resulting topography was analysed by confocal microscopy before and after the bend test.
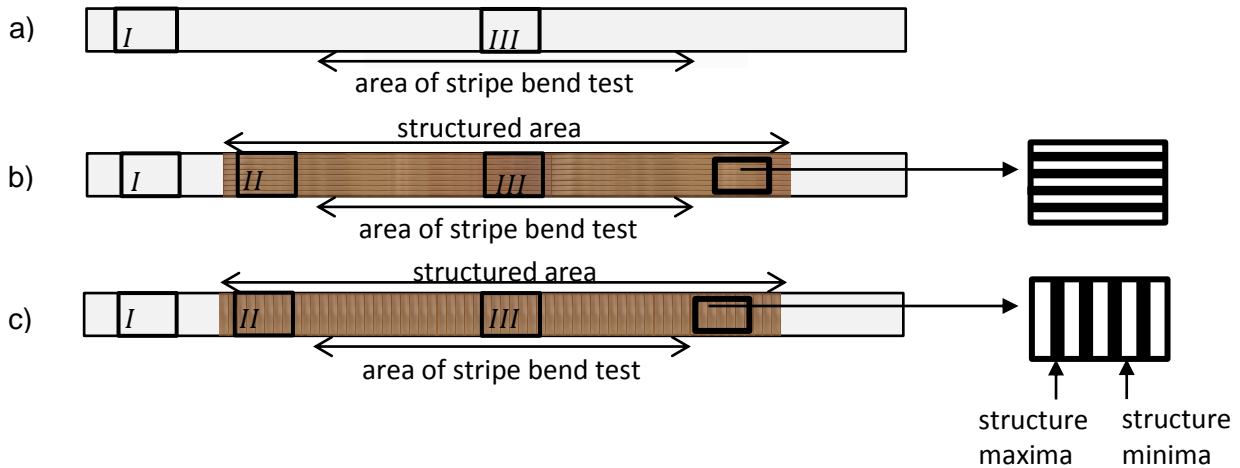
Fig. 3:   Unstructured reference strips a), longitudinal structured metal strips b) and transverse structured metal strips c) for draw bend test with areas for measurements: (**I**) reference surface, (**II**) structured surface without contact to bend rig, and (**III**) structured and bend surface.

2.2 Draw bend test

The tests were performed with a draw bend test machine under 90° deflection. The metal strips were clamped in around the function area of the draw-bend tool, see Figure 4. The 65 mm long and 10 mm thick cylindrical draw bend tools were made from cold work tool steel 1.2379 (X155CrVMo12-1, ASTM D2). The tools were coated with layers of tetrahedral amorphous carbon (ta-C) with different thicknesses. One group of tools has 4.25 µm thick ta-C layers, made with 1-fold tool rotation during deposition and the second group has 2.25 µm thick ta-C layers, deposited during 3-fold tool rotation during the deposition. The tests were carried out at room temperature under dry conditions with a constant drawing velocity of 100 mm/s and a contact surface pressure 50 MPa.
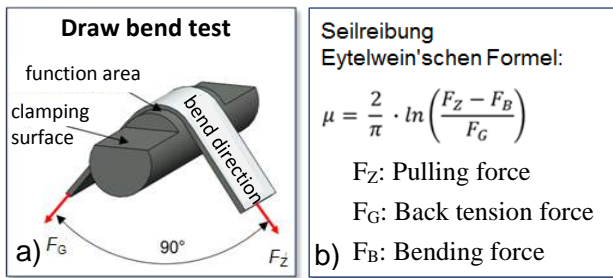

Fig. 4:   Scheme of the draw bend test setup. a) The metal strip is bend around the function area of the tool by 90° and pulled back and forth. b) Robe friction formula to calculate the coefficient of friction during the bend test

Following the test matrix, shown in Table 1, each tool group with a ta-C layer thickness of 4.25 µm or 2.25 µm uses 3 tools separately for a set of 21 of metal strips of non-structured references, with longitudinal DLIP-structures or transverse DLIP-structures or. Respectively 7 strips were used for one coated tool whereby each stripe had 400 mm deep drawn distance, made in one direction. Therefor the distance deep drawn over one tool sums up to 2800 mm.

Tab. 1:   Matrix of tools and metal strips. The tools differ in ta-C layer thickness (4.25 µm or 2.25 µm) and the metal strips are divided into groups with DLIP-structures longitudinal or transverse to bending direction or non-structured reference strips.

	Draw bend tools					
	1d rotated 4.25 µm ta-C thickness			3d rotated 2.25 µm ta-C thickness		
Sheet metal surface	3 tools + 21 strips un-structured	3 tools + 21 strips II structured	3 tools + 21 strips ⊢ structured	3 tools + 21 strips un-structured	3 tools + 21 strips II structured	3 tools + 21 strips ⊢ structured

3   Results

3.1   Surface characterization of metal strips

The metal strip surfaces were examined at several positions for statistical evaluation. Exemplary confocal images of the unstructured reference surface, the longitudinal structured surface and the transverse structured surface before the bend test are shown in (Figure 5 a-c).

The surface analysing was performed following the ISO 25178 standard on an area of 600 µm x 830 µm, which is related to the 20x confocal microscope objective. The unstructured reference surface shows an arithmetic surface roughness of Sa = 1.21 µm (Figure 5a).

On the structured strips, the initial surface topography is still present after the micro-structuring (Figure 5b and 5c). The DLIP - structures are following this initial surface topography, for longitudinal structuring as well as for transverse structuring, with a spatial period of 8 µm. Peak heights vary depending on the surface topography with maxima of up to 1.46 µm.
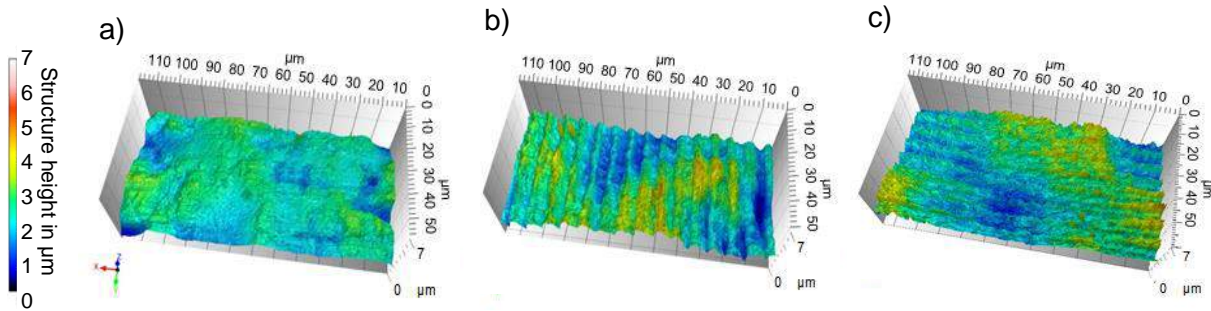
Fig. 5: Confocal images of the metal strip surfaces before the bend test, a) unstructured reference surface, b) longitudinal DLIP structures, c) transverse DLIP structures.
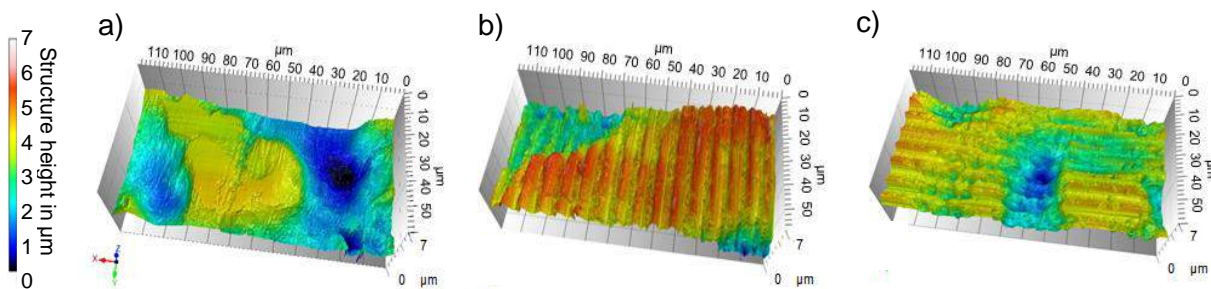

Fig. 6: Confocal images of the metal strip surfaces after the bend test, a) unstructured reference surface, b) longitudinal DLIP structures, c) transverse DLIP structures.

After carrying out the draw bend test, pieces of 20 mm x 20 mm were cut out from the strips to fit under the confocal microscope. Exemplary shown in Figure 6 a-c), fragments from the middle of the stripe with a low bend radius are chosen for the confocal analysis, see Position III Figure 3.

It can be seen, that the unstructured surface of the reference strips shows massive wear after bending. The former plateaus are abraded and the material volume of peaks (Vmp at area = 10%, ISO 25178) is similar to before the bend test (from 0.0462 µm³/µm² to 0.048 µm³/µm²).

The DLIP microstructures on the structured strips are still detectable after the bend test. In contrast to the unstructured surfaces, confocal images of the micro structured strips (Figures 6b and 6c) reveal a removal only at the maxima positions of the structured surface pattern on the initial surface plateaus. The DLIP structures in the topography valleys, lower than the contact level, show structure heights similar to those before the test, which means that these structures did not interact during the stripe bend test and did not show any friction and wear appearance. The Vmp of structured surfaces are nearly halved compared to before the bend test (from 0.0949 µm³/µm² to 0.0538 µm³/µm² for transverse structures and from 0.0617 µm³/µm² to 0.0366 µm³/µm² for longitudinal structures).

3.2 Influence of surface structuring on coefficient of friction during bend test

Figure 7 presents the coefficient of friction during the draw bend test of ta-C coated tools and unstructured or DLIP structured metal strips. It can be seen that the coefficient of friction is lower in bending test with 3-d

rotated tools compared to test with 1-d rotated tools. 3-d rotation during the carbon deposition leads to a homogenous layer thickness around the cylindrical bending tool and a higher homogeneity of the build in of following carbon atoms into the established ta-C layer. The ta-C layer thickness is 2.25 µm for 3d-rotated tools and 4.25 µm for 1-d rotated tools, measured at the tool function area (see Figure 4a).
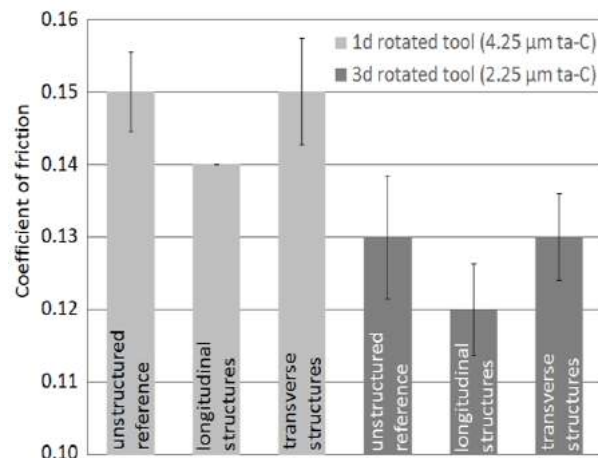

Fig. 7: Diagram of the coefficient of friction during draw bend test for reference and structured strip surfaces. The tools differ in ta-C layer thickness (1d = 4.25 µm, 3d = 2.25 µm) and the sheet metal strips in surface structuring (unstructured reference, longitudinal structures, transverse structures, see Figure 3).

Transverse metal strips seem not to lead to reduction in the coefficient of friction compared to unstructured reference surfaces. The coefficient of friction was µ = 0.15 with 1d-rotated tools and µ = 0.13 for 3d-rotated tools. This might be explained by the contact mechanism

between tool surface and metal strip surface during the bend test. The surface interacts with each DLIP structure aligned transverse to the bend direction over and over again anew, like a pouncing effect. This could be related to a newly interlocking of asperities from tool and structure peak for every peak, which leads to a higher coefficient of friction. A similar behavior can be seen with the surface of unstructured metal strips. The randomly distributed surface plateaus act like the transverse DLIP structure as a small barrier for the strip bending motion, which will be removed during the bending.

Furthermore, from Figure 7 it can be also seen that pairings with longitudinal structured metal strips lead to the lowest measured coefficients of friction with $\mu = 0.14$ with 1d-rotated tools and $\mu = 0.12$ with 3d-rotated tools, whereby the match of 3d-rotated tool and longitudinal structured metal strip has the lowest coefficient of friction in this test. The initial contact of the asperities of the tool and the DLIP-peaks happens only once. After the first contact, the tool surface slides on top of the peaks of the longitudinal structured metal strip in bending direction without having a repetitive new contact. This results in a smooth removal of surface asperities between tool and structure peaks. Additionally, only a small area of the tool is in contact with the metal strip. The area between two DLIP-structures is not removed, which leads to less friction and wear compared to unstructured surfaces.

4   Conclusions

Micro structured surfaces were produced by Direct Laser Interference Patterning on metal sheets to study the influence on lubricant free deep drawing processes. DLIP structures were applied on test metal strips longitudinal or transverse direction and tested with ta-C coated tools in a draw bend test rig. Non structured metal strips were also tested for reference purpose. The surfaces of the metal strips were characterized before and after the bending test, observing that the produced surface topographies were not significantly affected after the bending process. Only peaks on former surface plateaus were removed, whereby structures in surface valley are intact.

Considering the tribological performance during the bending test, it was observed that unstructured metal strips and transverse structured metal strips show similar coefficients of friction, independent from the usage of a 3d-rotated tool or a 1d-rotated tool. Longitudinal structured surfaces lead to a lower coefficient of friction than unstructured or transverse structured surfaces. An explanation for the observed phenomena can be related to the contact mechanism between tool surface and metal strip surface during bending. Surface asperities of unstructured or transverse structured metal strips interact with the tool asperities over and over again anew whereby the peaks of the longitudinal structures stay in contact with the tool surface during the bending. Moreover does the reduced contact area between tool surface and longitudinal DLIP structures support the reduction in friction and wear during bending.

References

[1]   M. Blaich, E. Dannenmann, E. Mössle: Tribologie der Blechumformung. In Lange. (Hrsg.): Umformtechnik, Band 3: Blechbearbeitung, Springer-Verlag (1990).

[2]   D.K. Karupannasamy, J. Hol, M.B. de Rooij, T. Meinders, D.J. Schipper: Modelling mixed lubrication for deep drawing processes, Wear p. 296-304 (2012).

[3]   S. Kataoka, M. Murakawa, T. Aizawa, H. Ike: Tribology of dry deep-drawing of various metal sheets with use of ceramics tools, Surface and Coatings Technology 177 –178, p. 582–590 (2004)

[4]   B. Lehmann, U. Litzinger: Vom Kühlschmierstoff zum Abwasser, Tribologie + Schmierungstechnik (1995).

[5]   K. Taube: Carbon-based coatings for dry sheet-metal working, Surface and Coatings Technology 1-3, p. 976-984 (1998).

[6]   W. Götz: Werkstücke schonend säubern und entfetten, Industrieanzeiger 42/95 (1995).

[7]   M. Rocker, I. Warfolomeow, G. Neumann: Regeln für Sicherheit und Gesundheitsschutz bei der Arbeit: Umgang mit Kühlschmierstoffen, BGR 143, Tribologie + Schmierungstechnik (2000).

[8]   F. Klocke, K. Gerschwiler: Minimalmengenschmierung – Systeme, Medien, Einsatzbeispiele und ökonomische Aspekte der Trockenbearbeitung, Trockenbearbeitung von Metallen, Proc. of the VDI-Seminar, Stuttgart, Mar. 18: 2.1-2.20. (2003).

[9]   K. Siegert, M. Ziegler, S. Wagner: Closed loop control of the friction force. Deep drawing process, Journal of Materials Processing Technology, p. 126-133 (1997).

[10]   l. Haas: Mit Bio-Ölen gut geschmiert?, VDI-Nachrichten, Nr. 34, p. 16+17 (2000).

[11]   M. Bieda, C. Schmädicke, T. Roch, A. Lasagni: Ultra-Low Friction on 100Cr6-Steel Surfaces After DirectLaser Interference Patterning, Adv. Eng. Mater. 17, 102 (2015).

[12]   M. Bieda, M. Siebold, A. F. Lasagni: Fabrication of Sub-Micron Surface Structures on Copper, Stainless. Steel and Titanium using Picosecond Laser Interference Patterning, Applied Surface Science 387, 175 (2016).

[13]   A. F. Lasagni, E. Beyer: Fabrication of periodic submicrometer and micrometer arrays using laser interference-based methods, Laser Surface Engineering, p. 423, Elsevier (2015).

[14]   R. Srinivasan, W.J. Leigh: Ablative photodecomposition: action of far-ultraviolet (193 nm) laser radiation on poly (ethylene terephthalate) films, Journal of the American chemical Society 104, p. 6784-6785 (1982).

[15]   G.B. Blanchet, Jr. C.R. Fincher: Laser induced unzipping: a thermal route to polymer ablation, Applied Physical Letters 65, p. 1311 (1994).

[16]   Y. Xia, G.M. Whitesides.: Soft lithography, Annual Review of Materials Science 28, p.153-184 (1998).

[17]   M. Geissler, Y. Xia, Patterning: principles and some new developments, Advanced Materials 16, No. 15 (2004).

[18]   F. Mücklich, A. Lasagni, C. Daniel: Laser interference metallurgy—periodic surface patterning and formation of intermetallics, Intermetallics 13, p. 437 (2005).

[19]   L. Longstreth-Spoor, J. Trice, H. Garcia, C. Zhang, R. Kalyanaraman: Nanostructure and microstructure of laser-interference-induced dynamic patterning of Co on Si J. Phys. D: Appl. Phys. 39, p. 5149 (2006).

[20]   M. K. Kelly, J. Rogg, C. E. Nebel, M. Stutzmann, S. Kátai: High-Resolution Thermal Processing of Semiconductors Using Pulsed-

Laser Interference Patterning phys. stat. sol. (a) 166, p. 651 (1998).

[21] A. F. Lasagni, T. Roch, J. Berger, T. Kunze, V. Lang, E. Beyer: To use or not to use (direct laser interference patterning), that is the question, SPIE LASE (Eds.: U. Klotzbach, K. Washio, C. B. Arnold), SPIE p. 935115 (2015).

[22] A. F. Lasagni, T. Roch, D. Langheinrich, M. Bieda, H. Perez, A. Wetzig, E. Beyer: Large area direct fabrication of periodic arrays using interference patterning, SPIE LASE (Eds.: F. G. Bachmann, W. Pfleging, K. Washio, J. Amako, W. Hoving, Y. Lu), SPIE p. 82440F (2012).

[23] V. Lang, T. Hoffmann, A. Lasagni: Optimization for high speed surface processing of metallic surfaces utilizing direct laser interference patterning, Proc. of SPIE 2018 (submitted).